Experimental investigations of laser beam image displacements in the turbulent atmosphere

V.M. Sazanovich and R.Sh. Tsvyk

Institute of Atmospheric Optics,
Siberian Branch of the Russian Academy of Sciences, Tomsk

Received October 4, 2004

The paper analyzes the results of experimental investigations into the laser beam propagation under conditions of developed convective turbulence over a heated surface with the Rayleigh number Ra ~ 10^8–10^{10}. The laser beam (λ = 0.63 μm) propagated at the height of 18, 25, and 36 cm above the surface. The path length was 2 m. The transmitter optical system generated a plane wave with the Gaussian intensity distribution. Laser beam displacements along the horizontal and vertical coordinates were measured simultaneously. The variance of displacements $\sigma_\alpha^2(2R)$, the correlation function $b(\tau)$, and the spectral density of fluctuations $fW(f)$ were calculated. The dependence of fluctuations of the image centroid on the detector diameter was determined at different heights above the surface.

Introduction

The propagation of laser radiation through a turbulent medium is accompanied by random distortions of the phase front of the wave, which, in their turn, lead to intensity fluctuations, beam wandering, and fluctuations of the image centroid. By now various aspects of radiation propagation through randomly inhomogeneous media have been considered quite thoroughly both theoretically and experimentally for the case of isotropic media, described by the Karman model of turbulence. The results of such investigations have been summarized in Refs. 1–4. However, quite often the medium is not isotropic due to various hydrodynamic instabilities and upward thermal flows over cities and fires.

The distortions of laser radiation in anisotropic media were discussed in Refs. 5–8. Some results of experimental investigations presented in Refs. 5 and 6, revealed the difference in the variances of beam wandering in the horizontal and vertical directions, as the beam propagated through a jet of a turbojet engine. Arsen'yan et al.[8] showed the anisotropy in the profiles of the beams, propagating over a city along a slant path in the presence of vertical flows.

In a homogeneous, isotropic turbulent medium, the variance σ_α^2 of random displacements of the image of a source of plane wave is determined through the structure function of phase fluctuations $D_s(\rho)$ and has the following form in the inertial range of the spectrum[1]:

$$\sigma_\alpha^2 = \frac{D_s(2R)}{4k^2R^2} = \frac{1}{\pi k^2R^2} \times$$

$$\times \int_0^{2R} \left[D_s''(\rho) + \frac{D_s'(\rho)}{\rho} \right] \left[\arccos\left(\frac{\rho}{2R}\right) - \frac{\rho}{2R}\sqrt{1-\left(\frac{\rho}{2R}\right)^2} \right] \rho d\rho; \quad (1)$$

$$D_s(\rho) = 2.84C_n^2k^2L(\rho)^{5/3} \text{ at } 2R \gg \sqrt{\lambda L}, \quad (2)$$

$$\sigma_{\alpha 0}^2(2R) = 2.84C_n^2L(2R)^{-1/3}, \quad (3)$$

where $k = 2\pi/\lambda$ is the wave number; λ is the wavelength; $2R$ is the detector diameter; L is the path length; ρ is the separation between the observation points; C_n^2 is the structure characteristic of the refractive index of the medium.

The boundary of the inertial range of the spectrum is determined by the inner scale of turbulence l_0 (about several millimeters) on the high-frequency side and by the outer scale L_0 on the low-frequency side. The outer scale L_0 depends on the height: $L_0 = \kappa_1 h$, where $\kappa_1 = 0.4$ is the Karman constant; h is the height at which the beam propagates over the surface. In Ref. 9 the boundaries of the inertial range were determined from the optical measurements of temporal fluctuations of the phase and the phase difference under conditions of developed turbulence along a 95 and 200-m paths. The spatial structure function of phase fluctuations $D_s(\rho) \approx \rho^{5/3}$ at the beam separation from 2–3 to 30–40 cm. At larger separations, phase fluctuations saturate. In the experiment, the laser beam propagated at the height of 1.5–2 m, that is, phase fluctuations saturated at the scales ~ $0.2h$ or ~ $0.5L_0$.

Note also that the dependence of the variance of phase fluctuations, calculated taking into account the outer scale, gives the slower and smoother saturation of $D_s(\rho)$ than it is observed in the experiment.[9] With the allowance made for the outer (energy) scale, the spectrum of refractive index fluctuations can be written in the form[4]:

$$F_\varepsilon(\kappa) = 0.32C_n^2\kappa^{-11/3}\left(1 + \frac{\kappa_0^2}{\kappa^2}\right)^{-11/6}, \quad (4)$$

where $\kappa = 2\pi/l$ is the wave number corresponding to the scale of turbulence l; $\kappa_0 = 2\pi/L_0$ is the wave

0235-6880/04/12 865-07 $02.00

number corresponding to the outer scale of turbulence L_0.

The variance σ_α^2 of random displacements of the image of a collimated beam, calculated taking into account the outer scale, can be written in the form[4]:

$$\sigma_\alpha^2(2R) = 2.84C_n^2L(2R)^{-1/3}\left[1-\left(1+\frac{2}{\kappa_0^2R^2}\right)^{-1/6}\right] =$$

$$= \sigma_{\alpha 0}^2\left[1-\left(1+\frac{2L_0^2}{\pi^2(2R)^2}\right)^{-1/6}\right]. \qquad (5)$$

Since the displacements of the centroid of the laser beam image depend on the scales of inhomogeneities comparable with the size of the receiving objective and larger, we can expect that experimental investigations of the source image jitter at the receiving aperture diameter close to the outer scale of turbulence L_0 will make it possible to determine the effect of the outer scale on the parameters of the radiation propagated.

This paper presents some results of experimental investigations on the propagation of laser radiation under conditions of developed convective turbulence over a heated surface.

Measurement technique

The experiments were conducted under laboratory conditions on a setup, modeling convective turbulence (randomly inhomogeneous medium over a heated surface). The surface dimensions were 2×1 m^2. The estimates of the Rayleigh number of the thermal flow over the surface showed that, depending on the input energy,

$$\mathrm{Ra} = \frac{g\beta h^3\Delta T}{\nu\chi} \approx 10^8 - 10^{10},$$

where g is the acceleration of free fall, cm/s^2; β is the temperature coefficient of volumetric expansion, 1/°C; ΔT is the temperature difference between the surface and the ambient medium, °C; ν is the kinematic viscosity coefficient, cm^2/s; χ is the thermal diffusivity, cm^2/s. That large values of the Rayleigh number are indicative of the developed turbulent motion over the surface.

The structure characteristic of the refractive index of the medium C_n^2, determined experimentally from optical measurements,[10] depends on the height above the surface $C_n^2 \approx C_{n0}^2(h/h_0)^{-4/3}$. In the atmosphere, such height dependence corresponds to the conditions of developed convection. The maximum values of C_{n0}^2 at the height $h_0 = 6$ cm achieve $\approx 10^{-10}$ cm$^{-2/3}$.

The laser beam ($\lambda = 0.63$ μm) propagated at the heights of 18, 25, and 36 cm above the surface. The path length in the turbulent medium was about 2 m. The appropriate optics was used to form a plane wave with the Gaussian intensity distribution and the effective radius $a_0 = 4$ cm. A receiving telescope with the focal length $F_t = 160$ cm and the diameter of 16 cm was used. Replaceable diaphragms with the diameters $d = 2R = 0.8$–11.6 cm were set in front of the receiving telescope. The displacements of the laser beam image along the horizontal, x, and vertical, y, coordinates were measured simultaneously using a device based on a dissector tracking system. The discretization frequency was 100 Hz. One realization consisted of 10000 readouts. The measured coordinates of the image centroid ($r_i = \sqrt{x_i^2 + y_i^2}$, x_i, y_i are the instantaneous values of the displacements measured) were used to calculate the variance of the image centroid displacements $\sigma_\alpha^2(2R)$. The correlation functions $b(\tau)$ and the spectral densities of the fluctuations $fW(f)$ were calculated for each coordinate.

Experimental findings

1. Variance of the displacements of the laser beam image

Figure 1 shows the experimentally obtained variance of the displacements of the laser beam image as a function of the diameter of the receiving objective. The detector diameter $2R$, normalized to the minimum diameter $2R_0 = 0.8$ cm, is plotted as the x axis, and the variance, normalized to that at the minimum diameter $2R_0$, is plotted as the y axis. Every point in the figure is obtained by averaging over 5–6 realizations under identical conditions. All the realizations measured at the three heights are characterized by a faster decrease of the variance of image jitter with the increasing diameter of the receiving objective than that following from Eq. (3).

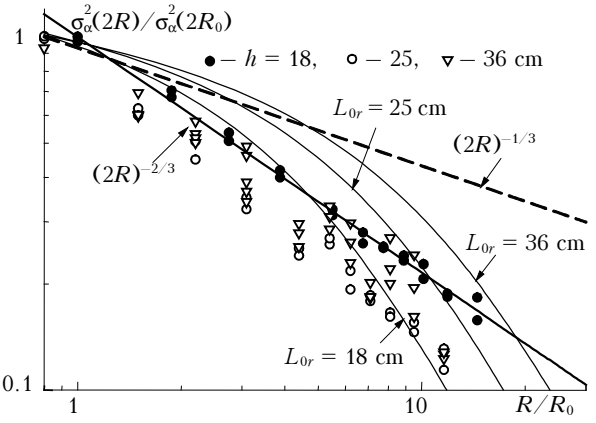

Fig. 1. Variance of fluctuations of the source image as a function of the receiving aperture diameter.

The approximation of the experimental results by Eq. (5), calculated with the outer scale of turbulence L_{0r} equal to the height of beam propagation above the surface h, is shown in Fig. 1 by thin curves. Equation (5) for each height is complemented with a constant coefficient so that the curves pass through

1 at $2R_0 = 0.8$ cm. The calculation by Eq. (5) using $L_{0r} \approx 0.4h$ gives a larger discrepancy with the experiment than for $L_{0r} \approx h$ (shown in Fig. 1). This could be expected if we take into account known measurement results on the spatial phase fluctuations, in which similar discrepancies between the experimental and calculated data were obtained. A satisfactory agreement is achieved in calculations[9] with the use of the dependence $L_{0r} \approx (0.6 \text{ to } 2)h$. The dashed line shows the dependence $\sigma_\alpha^2(2R) \sim (2R)^{-1/3}$ [Eq. (3)], corresponding to the homogeneous isotropic turbulence. The solid curve corresponds to the equation $\sigma_\alpha^2(2R) \sim (2R)^{-2/3}$, calculated by the least-squares method.

It can be seen from Fig. 1 that the experimental data are better described by the equation $\sigma_\alpha^2(2R) \sim (2R)^{-2/3}$ than by Eqs. (3) and (5). In this case, the structure function of the phase should have the form $D_s(\rho) \approx \rho^{4/3}$. The obtained dependence $\sigma_\alpha^2(2R) \sim (2R)^{-2/3}$ can be caused by the effect of the outer scale L_0, which, according to data from Ref. 9, can be $L_0 \approx 0.2h \sim 3$–8 cm. Note that only in a few experiments with small diameters there is a range, at which $\sigma_\alpha^2(2R) \sim (2R)^{-1/3}$.

In our experiment, the beam propagated in the developed convective flow over a heated surface. Since the height of laser beam propagation above the surface is less than the dimensions of the surface itself, the heat flux has a pronounced vertical direction at this height. Therefore, we should expect the differences in the outer scale values along the horizontal and vertical directions. This is seen in the levels of the image fluctuations measured along the coordinates x and y.

Figure 2 depicts the ratio of the root-mean-square fluctuations of the image of a laser source along two axes $\sigma_{\alpha y}/\sigma_{\alpha x}$ as a function of the detector diameter. Solid curves are the approximations by fourth-order equations, calculated by the least-squares method. These curves allow us to estimate the point of inflection in the experimental data.

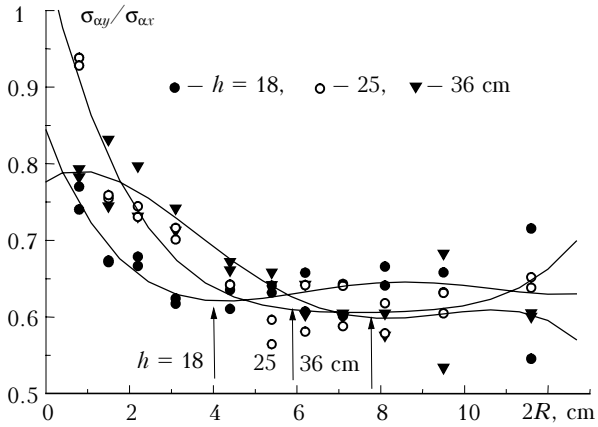

Fig. 2. Ratio of the root-mean-square fluctuations of the image $\sigma_{\alpha y}/\sigma_{\alpha x}$ as a function of $2R$ for different heights h.

It can be seen from Fig. 2 that once a certain value of the diameter (marked by arrows) is achieved for each height, the ratio $\sigma_{\alpha y}/\sigma_{\alpha x}$ changes its behavior. As this takes place, the spread of both the ratio $\sigma_{\alpha y}/\sigma_{\alpha x}$ and the values of $\sigma_{\alpha y}$ and $\sigma_{\alpha x}$ increase. The values of $\sigma_{\alpha y}/\sigma_{\alpha x}$ at the points of inflection for all heights are almost identical, and the ratio of the height of beam propagation to the objective diameter is almost identical as well, which is connected with the influence of the outer scale. We assume that the point of inflection correspond to the equality of the detector diameter and the outer scale. In this case, the outer scale takes the following values: $L_{0h1} \approx 4$ cm $\approx 0.22h_1$ at the height $h_1 = 18$ cm, $L_{0h2} \approx 6$ cm $\approx 0.24h_2$ at the height $h_2 = 25$ cm, and $L_{0h3} \approx 7.8$ cm $\approx 0.22h_3$ at the height $h_3 = 36$ cm. Similar ratios between L_0 and h were obtained in the experimental investigations of the spatial phase fluctuations.[9]

Figure 3 depicts the relation between the displacements $\sigma_{\alpha y}$ and $\sigma_{\alpha x}$ for different heights. It can be seen that at all the heights used in the experiment the horizontal displacements exceed the vertical ones.

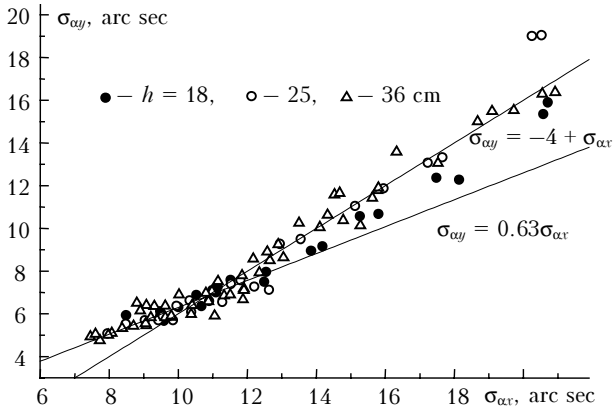

Fig. 3. Relation between the rms image fluctuations along the coordinates x and y.

The linear relation between the displacements along the coordinates x and y keeps true up to the angular displacements in the horizontal plane ~ 10–12 arc sec and is described by the function $\sigma_{\alpha y} = 0.63\sigma_{\alpha x}$, which corresponds to the points of inflection in Fig. 2. At the displacements $\sigma_\alpha^2 \geq 10$–12 arc sec ($h/2R \geq 4$, which corresponds to small diaphragms) the tangent of the angle of slope of the straight line describing the relation between $\sigma_{\alpha y}$ and $\sigma_{\alpha x}$ increases to 1, and the linear relation between the displacements along the axes x and y is described by the equation $\sigma_{\alpha y} = -4 + \sigma_{\alpha x}$. This is indicative of the homogeneity of the fluctuations of the refractive index at $2R \leq 3$–5 cm.

The alternation of the relation between $\sigma_{\alpha y}$ and $\sigma_{\alpha x}$ at the receiving aperture diameter $2R \geq 3$–5 cm can have two opposite explanations. First, as follows from Eq. (5), an increase in the outer scale leads to an increase of the displacements. Therefore, in the region where $\sigma_{\alpha y} = 0.63\sigma_{\alpha x}$, the horizontal outer scale

should be larger than the vertical one $L_{0x} \geq L_{0y}$. Second, at the smaller outer scale, its variations can play a greater role. Outside the region of homogeneous turbulence (where $\sigma_{\alpha y}$ and $\sigma_{\alpha x}$ are equal and C_n^2 is homogeneous), the gradient of fluctuations of the refractive index should increase in the direction of the smaller scale. Both these factors can lead to an increase of the displacements $\sigma_{\alpha x}$ and, as a consequence, to $\sigma_{\alpha y} < \sigma_{\alpha x}$. In this case, the horizontal scale should be smaller than the vertical one $L_{0x} \leq L_{0y}$. Further analysis of the spectra and correlation functions showed that the second assumption is preferable, although the data are quite contradictory.

2. Temporal autocorrelation functions and spectra of fluctuations of the image displacements

Figure 4 shows an example of the temporal autocorrelation functions of the normalized time τ/τ_0 for two height values. Here τ_0 is the correlation time, determined from the values of the autocorrelation function at the level $1/e$. Figure 4 shows the times τ_{0x} and τ_{0y} for the coordinates x and y. The autocorrelation functions along the axis x cross the zero line at larger values of τ/τ_0. Figure 5 shows the correlation time, determined by the $1/e$ and 0.1 levels of the correlation function, versus $2R$.

It can be seen from Figs. 4 and 5 that all correlation functions almost coincide at $\tau < \tau_0$ and differ significantly at $\tau > \tau_0$. The correlation time τ_0 increases proportionally to d. The equations of the straight lines, approximating experimental results (Fig. 5*a*) are: (*1*) $\tau_{0x} = 0.04 + 0.074(2R)$; (*2*) $\tau_{0y} = 0.04 + 0.06(2R)$; (*3*) $\tau_{0x} = 0.02 + 0.025(2R)$; (*4*) $\tau_{0y} = 0.052 + 0.02(2R)$. The correlation time along the vertical coordinate increases roughly threefold as slow as that along the horizontal one does. Along the horizontal coordinate, τ_0 saturates at the diameter $2R \approx 8.1$ cm at the height of 18 cm and $2R \approx 5.4$ cm at the height of 36 cm (marked by arrows in Fig. 5*a*). Along the vertical axis, there is no obvious saturation, but the tendency toward saturation is observed. At the $\tau_{0.1}$ level, the correlation increases with the increase of the detector diameter (Fig. 5*b*).

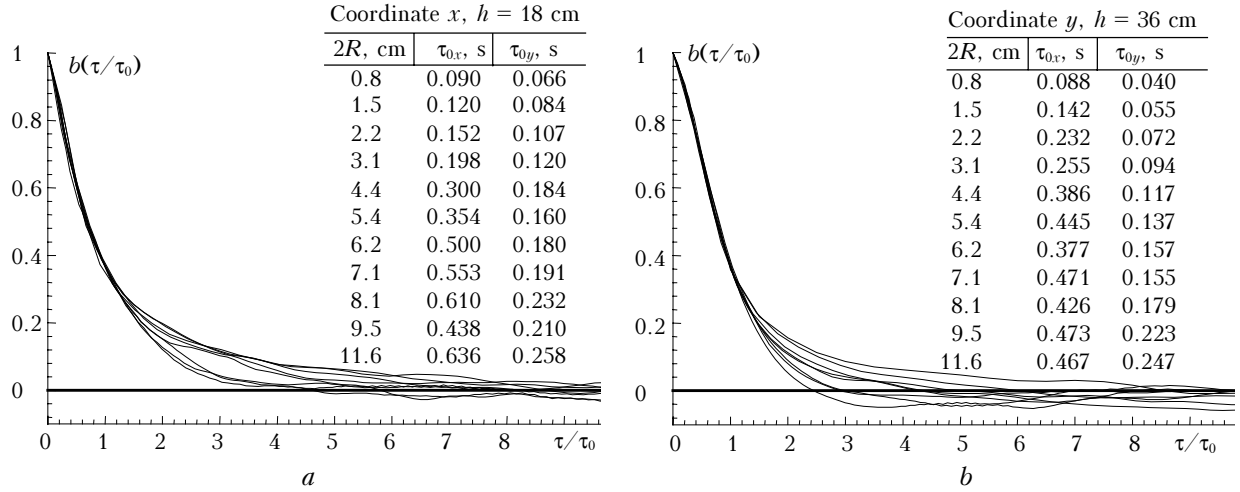

Fig. 4. Temporal autocorrelation functions of fluctuations of the image displacements at $h = 18$ (*a*) and 36 cm (*b*) at different $2R$.

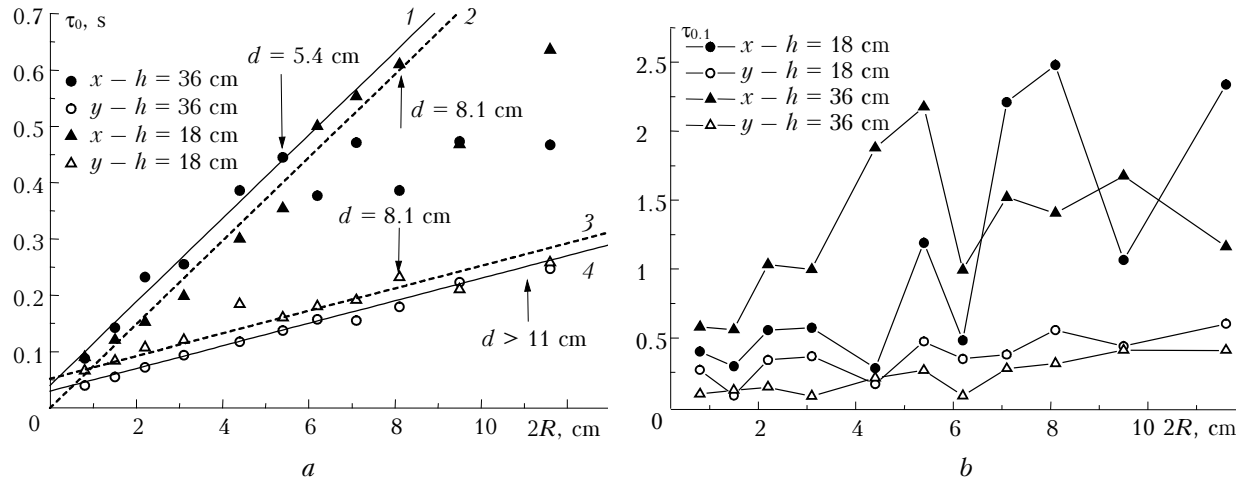

Fig. 5. Correlation time (τ), determined at $1/e$ level (τ_0) (*a*) and 0.1 level ($\tau_{0.1}$) (*b*) vs. $2R$.

The correlation time along the coordinate x fluctuates strongly at all heights. This behavior of correlation functions means that the spectrum of image displacements changes with the increasing diameter. The role of low frequencies increases, and, as a consequence, the displacements along the horizontal coordinate increase.

As an example, Fig. 6 shows the spectra of image displacements at the height of 18 cm for different detector diameters. The straight lines $U(f) = fW(f) \sim f^{-5/3}$, $U(f) \sim f^{1/2}$, and $U(f) \sim f$ describe the asymptotic forms of the spectrum in the regions of high and low frequencies.

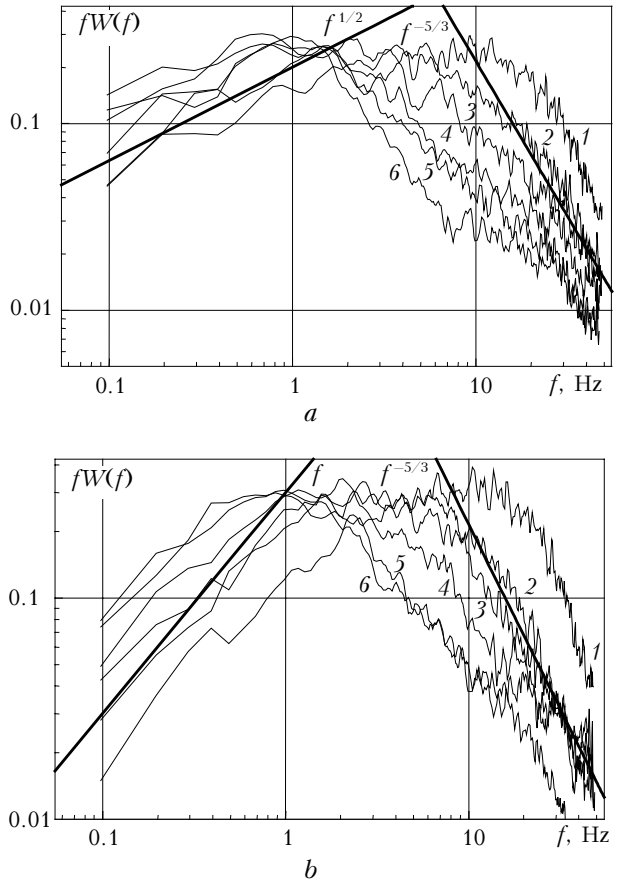

Fig. 6. Spectral densities of the image displacements at the height h = 18 cm along the axis x (*a*) and axis y (*b*) at d = 0.8 (*1*), 2.2 (*2*), 3.1 (*3*), 5.4 (*4*), 9.5 (*5*), and 11.6 cm (*6*).

It can be seen that with the increase of the detector diameter the spectrum shifts toward low frequencies. At the same time, in the region of high frequencies there is a part $U(f) \sim f^{-5/3}$, corresponding to the asymptotics of the theoretical spectrum. In the region of low frequencies the spectrum along the coordinate x increases in accordance with the theoretical one $U(f) \sim f^{1/2}$, while that along the coordinate y increase as $U(f) \sim f^{0.85}$. With the detector diameter greater than 3 cm, the spectrum along the horizontal coordinate x changes more significantly than that along the vertical coordinate does.

Figure 7 shows the dependence of the frequency determined at the $U(f)/e$ level in the region of high frequencies. It can be seen that the frequency decreases with the increase of the detector diameter following the power law. This decrease is faster along the horizontal than along the vertical, which can be connected with the influence of the outer scale on the averaging effect of the receiving aperture.

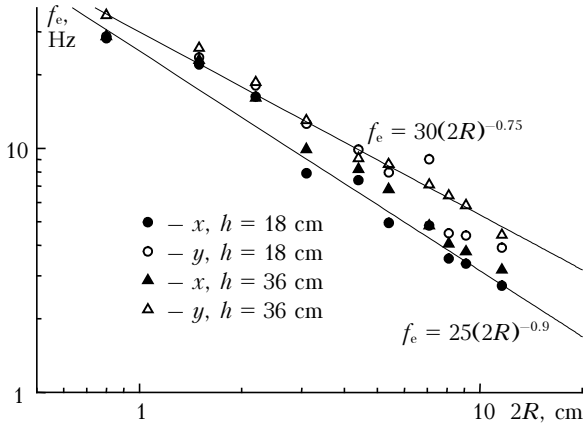

Fig. 7. Frequency of the spectrum determined at the $U(f)/e$ level in the high-frequency region vs. $2R$.

It is known[1] that the maximum of the spectrum in the inertial range is $f_0 \sim V_\perp/d$, then $f/f_0 = fd \sim V_\perp$ ($V_\perp$ is the velocity of transfer of inhomogeneities across the diaphragm). Analysis of the dependence of $U(f)$ on fd (Figs. 8*a* and *b*) showed that with the increase of the detector diameter the spectra do not coincide completely. The best agreement between the spectra was obtained when the dependence of the frequency on the detector diameter was taken into account (Figs. 8*c* and *d*). In these figures, $fd^{-0.9}/0.3V$ is plotted as a frequency for the displacements in the horizontal plane (coordinate x), while $fd^{-0.75}/0.3V$ is plotted for the coordinate y. The measurements of the wind velocity carried out with a thermoanemometer showed that it does not exceed 25–30 cm/s. The results of such processing are shown in Fig. 8.

The correlation function and the spectrum of phase fluctuations with the allowance made for the outer scale (4) have the form[3]:

$$b(\rho) = A_1\left(\frac{\kappa_0\rho}{2}\right)^{5/6} K_{-5/6}(\kappa_0\rho);$$

$$W(\kappa) = A\kappa\kappa_0^{-1}\left(1 + \frac{\kappa^2}{\kappa_0^2}\right)^{-4/3}, \qquad (6)$$

where $K_{-5/6}(\kappa_0\rho)$ is the McDonald function.

Similar function can also be written for the temporal spectrum of the image displacements, where $f_{01} \sim V_\perp/L_0$:

$$fW(f) = A\frac{f}{f_{01}}\left(1 + \frac{f^2}{f_{01}^2}\right)^{-4/3}. \qquad (7)$$

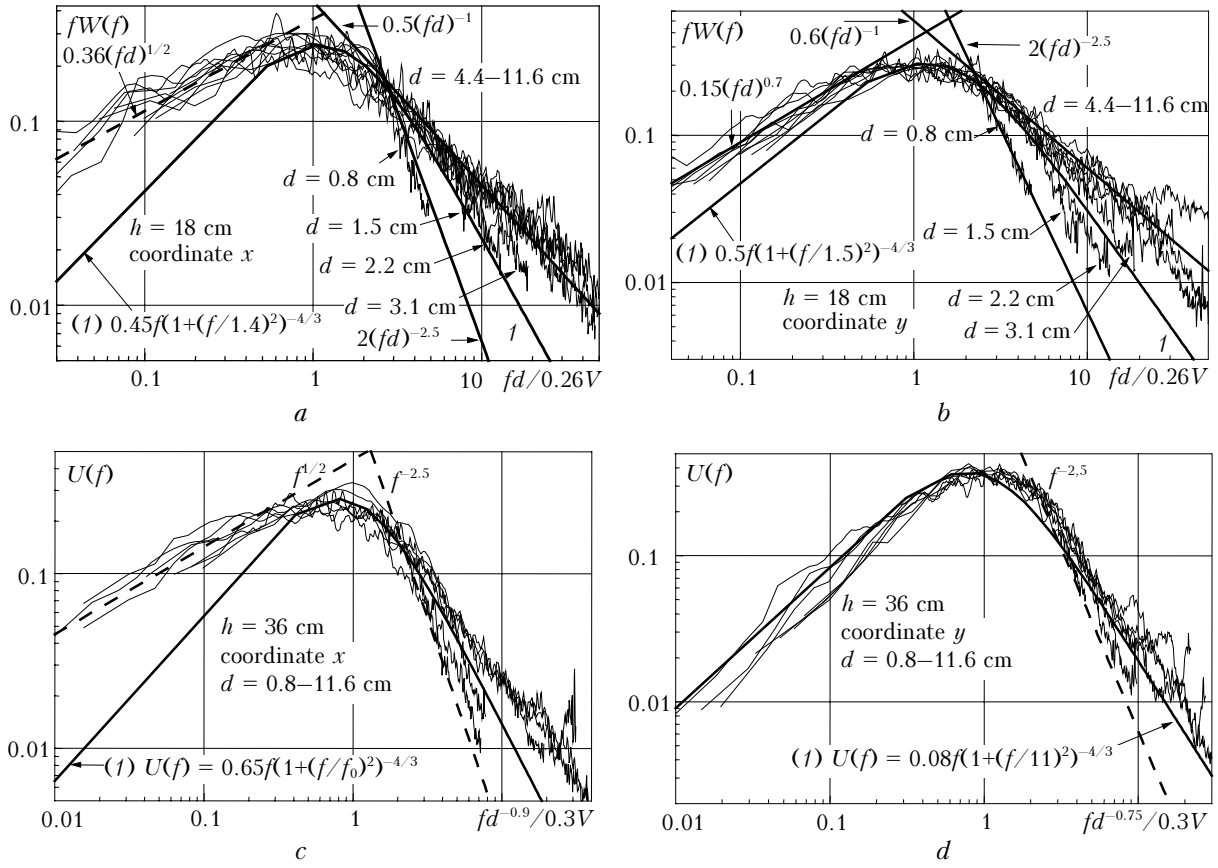

Fig. 8. Average spectra of the image displacements vs. normalized frequency. Curves *1* show data calculated by Eq. (7).

Figure 8 shows the spectra (curves *1*) calculated by this equation. The values of f_{01} were fitted based on the experimental data. From these data we can see that Eq. (7) rather well describes the spectrum of the displacements along the coordinate y. With the increase of the detector diameter, the spectrum extends to the high-frequency region. Almost all spectra include a part, where $U(f) \sim f^{-5/3}$.

Conclusions

1. The variance of fluctuations in the displacements of a laser beam image centroid decreases as $\sigma^2(2R) \approx (2R)^{-2/3}$ in place of $\sigma^2(2R) \approx (2R)^{-1/3}$, which is applicable in the inertial range (see Fig. 1). This dependence can be attributed to the influence of the outer scale.

2. The temporal autocorrelation functions normalized to τ_0, determined at the e^{-1} level, are close to each other (see Fig. 4). This confirms the known fact that the correlation time is determined by the detector diameter and the medium transfer rate. The spread in the values of the correlation function is significant in the region of large τ and small in the region of small τ.

3. The correlation time τ_0 along the horizontal coordinate is much larger than that along the vertical one. It increases proportionally to the detector diameter, but 2.5 times faster along the axis x. This can be explained by the anisotropy of turbulence above the heated surface. However, we failed to find an explicit relation between the horizontal and vertical scales (L_{0x} and L_{0y}).

4. The shapes of the spectra significantly depend on the detector diameter both in the low-frequency and high-frequency regions. The high-frequency region includes the spectral parts with the slope $\sim f^{-5/3}$ and $\sim f^{-1}$. With the increase of the detector diameter, the part $\sim f^{-5/3}$ decreases, while the part $\sim f^{-1}$ increases.

5. The maxima of the frequency spectra coincide at $f_m(2R) \approx 0.3V/d^{\alpha}$, where $\alpha = 0.9$ for the horizontal coordinate and 0.75 for the vertical coordinate.

References

1. V.I. Tatarskii, *Wave Propagation in a Turbulent Medium* (McGraw Hill, New York, 1961).
2. V.E. Zuev, V.A. Banakh, and V.V. Pokasov, *Optics of the Turbulent Atmosphere* (Gidrometeoizdat, Leningrad, 1988), 270 pp.
3. A.S. Gurvich, A.I. Kon, V.L. Mironov, and S.S. Khmelevtsov, *Laser Radiation in the Turbulent Atmosphere* (Nauka, Moscow, 1976), 278 pp.
4. V.L. Mironov, *Laser Beam Propagation in the Turbulent Atmosphere* (Nauka, Novosibirsk, 1981), 246 pp.

5. V.S. Sirazetdinov, D.I. Dmitriev, I.V. Ivanova, and D.H. Titterton, Atmos. Oceanic Opt. **14**, No. 10, 824–829 (2001).
6. V.S. Sirazetdinov, D.I. Dmitriev, I.V. Ivanova, and D.H. Titterton, Atmos. Oceanic Opt. **14**, No. 10, 830–834 (2001).
7. E.3. Gribova and A.I. Saichev, Atmos. Oceanic Opt. **14**, No. 10, 814–817 (2001).
8. T.I. Arsen'yan, A.M. Zotov, P.V. Korolenko, M.S. Maganova, and A.V. Mesnyankin, Atmos. Oceanic Opt. **14**, No. 10, 818–823 (2001).
9. V.P. Lukin, V.L. Mironov, V.V. Pokasov, and S.S. Khmelevtsov, Radiotekhn. i Elektron. **20**, No. 6, 1164–1170 (1975).
10. V.A. Banakh, V.M. Sazanovich, R.Sh. Tsvyk, and B.N. Chen, Atmos. Oceanic Opt. **9**, No. 12, 1033–1036 (1996).